

Critical behavior of the two-dimensional random-bond Potts model: A short-time dynamic approach

J. Q. Yin,¹ B. Zheng,^{1,2} and S. Trimper²

¹*Zhejiang University, Zhejiang Institute of Modern Physics, Hangzhou 310027, China*

²*Fachbereich Physik, Universität-Halle, 06099 Halle, Germany*

(Received 28 July 2004; published 29 November 2004)

The short-time critical dynamics of the two-dimensional eight-state random-bond Potts model is investigated with large-scale Monte Carlo simulations. Dynamic relaxation starting from a disordered and an ordered state is carefully analyzed. The continuous phase transition induced by disorder is studied, and both the dynamic and static critical exponents are estimated. The static exponent β/ν shows little dependence on the disorder amplitude r , while the dynamic exponent z and static exponent $1/\nu$ vary with the strength of disorder.

DOI: 10.1103/PhysRevE.70.056134

PACS number(s): 64.60.Fr, 05.50.+q, 75.40.Mg, 64.60.Ht

I. INTRODUCTION

The effect on the critical behavior of adding quenched disorder to statistical systems has been intensively investigated in the last two decades, both theoretically and numerically. According to the earlier works [1–4], quenched disorder could produce rounding of a first-order phase transition and thus induce a second-order one. Along this understanding, many activities in the last years have been devoted to the random-bond Potts (RBP) model and some variants [5–27]. It is exactly known that the pure two-dimensional (2D) Potts model undergoes a first-order transition for $q > 4$, while a continuous one for $q \leq 4$. Therefore, the 2D RBP model serves as a good laboratory for examining the effect of disorder. For a review of the Potts model, see Ref. [28].

A decade ago, Chen, Ferrenberg, and Landau performed a Monte Carlo simulation of the 2D eight-state RBP model. A second-order phase transition was observed. From the numerical values of the critical exponents, the 2D RBP model was believed to be in the same universality class as the pure 2D Ising model [5,6]. Similar conclusions were obtained for the random-bond Ashkin-Teller model, four-state RBP model and random-bond Ising model [7]. There is also experimental evidence claiming the same for the four-state Potts model [8].

However, contradictive results were obtained by Ludwig [9] and Dotsenko *et al.* [10]. It was argued with renormalization group methods that a new random-bond fixed point exists for $q > 2$, whose critical behavior is not Ising like. Later, Chatelain and Berche [27] performed numerical simulations for the self-dual eight-state RBP model and observed that the exponents γ/ν and β/ν are quite different from the Ising values, but close to Cardy and Jacobsen's prediction with the transition matrix method [13]: that β/ν varies continuously with q and ν changes only weakly. From the numerical simulations of the five-state RBP model, the magnetic exponent also indicates a new universality class [14]. In the case of the three-state RBP model, whose pure version exhibits a continue phase transition, Monte Carlo simulations [15,16] suggest that while the ratios γ/ν and β/ν do not change significantly, the exponent ν changes continuously with the strength of disorder. A recent numerical study of the

RBP model [17] gives q -dependence critical exponents, consistent with that obtained with the transition matrix method [22]. *To summarize*, the above analytical and numerical results support that the exponent ν varies continuously with the strength of disorder, while β/ν is more or less independent of the strength of disorder. Both exponents suggest that the 2D RBP model is not in the same universality class as the 2D Ising model.

On the other hand, it is interesting and important to investigate the effect of disorder on critical dynamics. The spin-glass dynamics is a very important example. However, the critical slowing down in numerical simulations of spin glasses is so severe that we hardly simulate large lattices. The RBP model may be a good model system for understanding the slow dynamics of disordered systems. Traditionally, it was believed that universal dynamic scaling behavior only exists in the long-time regime of the dynamics evolution. However, numerical simulations of the critical dynamics of the RBP model in the long-time regime are not easy. Little progress has been achieved in this direction.

In 1998, with renormalization group methods Janssen, Schaub, and Schmittmann derived a dynamic scaling form for the $O(N)$ vector model, which is valid up to the *macroscopic short-time regime*, after a microscopic time scale t_{mic} [29]. The dynamic process they considered is that the system initially at a very high temperature state with a small or zero magnetization is suddenly quenched to the critical temperature and then released to dynamic evolution of model A. It is important that a new independent critical exponent θ be introduced to describe the scaling behavior of the initial magnetization. Such a short-time dynamic scaling behavior has been numerically verified [30–34], and it is also consistent with relevant theories and experiments in spin glasses [30,35,36]. In spin glasses, the remanent magnetization corresponds to the autocorrelation function in the regular Ising systems without disorder. Furthermore, the short-time dynamic scaling can be extended to the dynamic relaxation starting from an ordered state [32,37,38].

More interestingly, based on short-time dynamic scaling, it is possible to extract not only the dynamic exponents, but also the static exponents as well as the critical temperature [32,39–41]. Since the measurements are carried out in the

short-time regime of the dynamic evolution, the method does *not* suffer from a critical slowing down. What we pay for this approach is that the measurements of the dynamic exponents and static exponents cannot be separated. Therefore, the statistical errors of the static exponents include those from the dynamic exponents. However, if we are also interested in the dynamic behavior, the short-time dynamic approach is rather useful.

A first numerical study based on the short-time dynamic approach suggests that the critical dynamic behavior of the 2D RBP model appears also not in the universality class of the 2D Ising model [18]. However, the numerical simulations are not very systematic and complete. The updating time is limited to 300 or 500 Monte Carlo time steps, which is not sufficiently long for a slow dynamics with disorder. The obtained exponents are not so accurate, and especially, the estimate of the exponent θ looks problematic. The probable reason is that the exponent θ may not be estimated by measuring the maximum magnetization of its eight components in the nonequilibrium state.

The purpose of this article is to present a systematic study of the short-time critical dynamics of the eight-state random-bond Potts model in two dimensions. We will perform simulations up to 150 000 Monte Carlo time steps, carefully analyze the dynamic scaling behavior, and provide relatively accurate measurements of the critical exponents. We show that the dynamic exponent z and the static exponent $1/\nu$ vary with the strength of disorder.

The models and scaling analysis of the dynamic behavior are described in Sec. II. Numerical simulations are presented in Sec. III. The final section contains the conclusions.

II. MODEL AND DYNAMIC SCALING BEHAVIOR

A. Random-bond Potts model

The Hamiltonian of the two-dimensional q -state Potts model with quenched random interactions can be written as

$$-\frac{1}{k_B T} H = \sum_{\langle i,j \rangle} K_{ij} \delta_{\sigma_i, \sigma_j}, \quad K_{ij} > 0, \quad (1)$$

where the spin σ takes the values $1, \dots, q$, δ is the Kronecker delta function, and the sum is over nearest-neighbor pairs on a two-dimensional square lattice. The dimensionless couplings K_{ij} are selected from positive values of K_1 and $K_2 = rK_1$, with a strong to weak coupling ratio $r = K_2/K_1$ called the *disorder amplitude*, according to a bimodal distribution

$$P(K) = p\delta(K - K_1) + (1 - p)\delta(K - K_2). \quad (2)$$

For $p=0.5$, the system is *self-dual* and the exact critical point can be determined by [42]

$$(e^{K_{1c}} - 1)(e^{K_{2c}} - 1) = q, \quad (3)$$

where K_{1c} and K_{2c} are the corresponding critical values of K_1 and K_2 , respectively. The case of $r=1$ corresponds to the pure Potts model, and the critical point is located at $K_c = \ln(1 + \sqrt{q})$. With an additional random-bond distribution, however, new second-order phase transitions are induced for any of the q -state Potts models and the new critical points are

determined according to Eq. (3) for different values of the disorder amplitude r and state parameter q .

In this paper, we study the self-dual case ($p=0.5$) of the eight-state random-bond Potts model with the short-time dynamic approach. Monte Carlo simulations with a standard Metropolis algorithm are performed on a two-dimensional square lattices with periodic boundary conditions. For a review of the short-time critical dynamics and its applications, see Refs. [32,39].

The physical observables we measure are the time-dependent magnetization, its second moment, autocorrelation, and spatial correlation of the q -state Potts model, respectively, defined as

$$M(t) = \frac{q}{(q-1)L^2} \left\langle \sum_i \left(\delta_{\sigma_i(t), 1} - \frac{1}{q} \right) \right\rangle, \quad (4)$$

$$M^{(2)}(t) = \frac{q^2}{(q-1)^2 L^4} \left\langle \left[\sum_i \left(\delta_{\sigma_i(t), 1} - \frac{1}{q} \right) \right]^2 \right\rangle, \quad (5)$$

$$A(t) = \frac{1}{L^2} \left\langle \sum_i \left(\delta_{\sigma_i(0), \sigma_i(t)} - \frac{1}{q} \right) \right\rangle, \quad (6)$$

$$C(x, t) = \frac{1}{L^2} \left\langle \sum_i \left(\delta_{\sigma_i(t), \sigma_{i+x}(t)} - \frac{1}{q} \right) \right\rangle, \quad (7)$$

where L is the lattice size.

B. Quench with ordered start

For a dynamic process quenched from a completely ordered state (an ordered start)—i.e., the initial magnetization $m_0=1$ —we assume a universal dynamic scaling form in the *macroscopic short-time* regime. For the k th moment of the magnetization, for example,

$$M^{(k)}(t, \tau, L) = b^{-k\beta/\nu} M^{(k)}(b^{-z}t, b^{1/\nu}\tau, b^{-1}L), \quad k = 1, 2. \quad (8)$$

Here $\tau = (K_1 - K_{1c})/K_{1c}$, and β , ν are the well-known static critical exponents, z is the dynamic exponent, and b is an arbitrary scale factor. This dynamic scaling form looks the same as that in equilibrium or close to equilibrium, but now it is expected to hold already when the dynamic system is still far from equilibrium, after a time scale t_{mic} which is long enough in the microscopic sense. t_{mic} is not universal. It is only a few Monte Carlo time steps for some simple dynamic systems, while can be hundreds or thousands of Monte Carlo time steps for slow dynamics.

In general, for determination of the dynamic exponent z and static exponents, a dynamic process starting from a completely *ordered* state can be more favorable than starting from a completely disordered state, since the statistical fluctuation is somewhat less, and especially the nonzero magnetization can be used for the scaling analysis. Assuming that the lattice is sufficiently large, the dynamic scaling form of the magnetization $M(t) \equiv M^{(1)}(t)$ around the critical point is written as

$$M(t, \tau) = t^{-c_1} F(t^{1/\nu z} \tau), \quad c_1 = \beta/\nu z. \quad (9)$$

If $\tau=0$, the magnetization decays by a power law $M(t) \sim t^{-c_1}$. If $\tau \neq 0$, the power-law behavior is modified by the scaling function $F(t^{1/\nu z} \tau)$. From this fact, one determines the critical point and the critical exponent $\beta/\nu z$. To estimate the exponent $1/\nu z$, we differentiate $\ln M(t, \tau)$ and obtain

$$\partial_\tau \ln M(t, \tau)|_{\tau=0} \sim t^{c_1}, \quad c_1 = 1/\nu z. \quad (10)$$

In order to estimate the dynamic exponent z *independently*, we introduce a Binder cumulant $U = M^{(2)}/M^2 - 1$, and the finite-size scaling analysis shows that at the transition point

$$U(t, L) \sim t^{c_2}, \quad c_2 = d/z. \quad (11)$$

From Eqs. (9)–(11), we are able to extract all the static exponents β and ν and the dynamic exponent z , which are originally defined in equilibrium. The attractive feature of the short-time dynamic approach is that we may *predict* all these exponents at the beginning of the time evolution and therefore do not suffer from a critical slowing down.

C. Quench with disordered start

For a dynamic process quenched from a completely disordered state (a disordered start) with a zero or *small* initial magnetization m_0 , a generalized dynamic scaling form can be written down, e.g., for the k th moment of the magnetization:

$$M^{(k)}(t, \tau, m_0, L) = b^{-k\beta/\nu} M^{(k)}(b^{-z} t, b^{1/\nu} \tau, b^{x_0} m_0, b^{-1} L), \quad k = 1, 2. \quad (12)$$

Here x_0 is an independent exponent describing the scaling behavior of m_0 , and it can be expressed with another exponent θ as

$$x_0 = \beta/\nu + \theta z. \quad (13)$$

Two interesting observables in this process are the autocorrelation and the second moment of the magnetization. For $\tau=0$ and $m_0=0$, it is well known that [30,32]

$$M^{(2)}(t) \sim t^\nu, \quad \nu = (d - 2\beta/\nu)/z. \quad (14)$$

Careful analysis reveals [35] that the autocorrelation at the transition point behaves like

$$A(t) \sim t^{-\lambda}, \quad \lambda = \frac{d}{z} - \theta. \quad (15)$$

Interesting here is that even though $m_0=0$, the exponent θ still enters the autocorrelation. The behavior in Eq. (15) has been confirmed in a variety of statistical systems [30,32].

In principle, one may also determine the exponent $1/\nu z$ from Eq. (12) in a way described in the preceding subsection. However, the fluctuation here is larger.

Similarly, the scaling behavior of the equal-time spatial correlation function at $\tau=0$ is

$$C(x, t) \sim t^{-2\beta/\nu z} C(x/t^{1/z}, 1). \quad (16)$$

The dynamic exponent z and static exponent β/ν can be also extracted from the data collapse of $C(x, t)$. This needs, how-

ever, a very large lattice and sufficient samples for an average.

Finally, to extract the exponent θ independently, we may consider a small but nonzero initial magnetization m_0 . From the dynamic scaling in Eq. (12), it is easy to deduce that the magnetization in the short-time regime obeys a power law

$$M(t, m_0) \sim m_0 t^\theta. \quad (17)$$

In many cases, the exponent is positive; i.e., the magnetization undergoes a critical initial increase. In the past decade, this phenomenon has been intensively discussed both theoretically and numerically. Usually, this behavior can be easily detected in Monte Carlo simulations. In the presence of disorder, however, this may not be the case.

III. NUMERICAL SIMULATIONS

We have performed Monte Carlo simulations with the standard Metropolis algorithm. Taking into account the slow dynamics induced by disorder and the effect of crossover from the pure Potts model to with disorder, the maximum updating time is taken to be from 10 000 to 150 000 Monte Carlo time steps, depending on the strength of disorder and the initial conditions. The results are presented with a lattice size $L=280$. To investigate the possible finite-size effects, some simulations have been also performed for $L=140$. Samples of the initial configuration for averaging are from 5000 to 10 000. To estimate the errors, samples are divided into some subgroups. In addition, errors induced by fluctuations along the time direction are also taken into account.

A. Continuous phase transition

Aizenman and Wehr [4] have rigorously proved that quite generally for $d \leq 2$ an *arbitrarily* weak amount of quenched bond randomness leads to elimination of any discontinuity in the density of the variable conjugate to the fluctuating parameter, but the signal of the continuous phase transition is difficult to be detected in the weak disorder regime for a finite lattice size. There seems to exist a finite-size-dependent threshold value of the quenched disorder amplitude r [43].

This fact is also reflected in the dynamic processes. For a small value of r , the dynamic system looks like it is undergoing a first-order phase transition. For a lattice size $L=280$ and a maximum updating time 10 000, the threshold value is about $r_c=1.30$. For $r > r_c$, the typical behavior of a second-order phase transition can be observed. For example, the relevant observables exhibit a power-law behavior at the transition temperature *independent of the initial conditions*. This is shown for $r=3$ in Fig. 1. According to Schülke and Zheng [44], this fact provides a evidence that a second-order phase transition is induced.

In other words, one will not observe any power-law behavior if the phase transition is a standard first-order one. If the first-order transition is weak, an approximate power-law behavior may appear at a certain temperature, but this pseudocritical temperature is initially condition dependent [44].

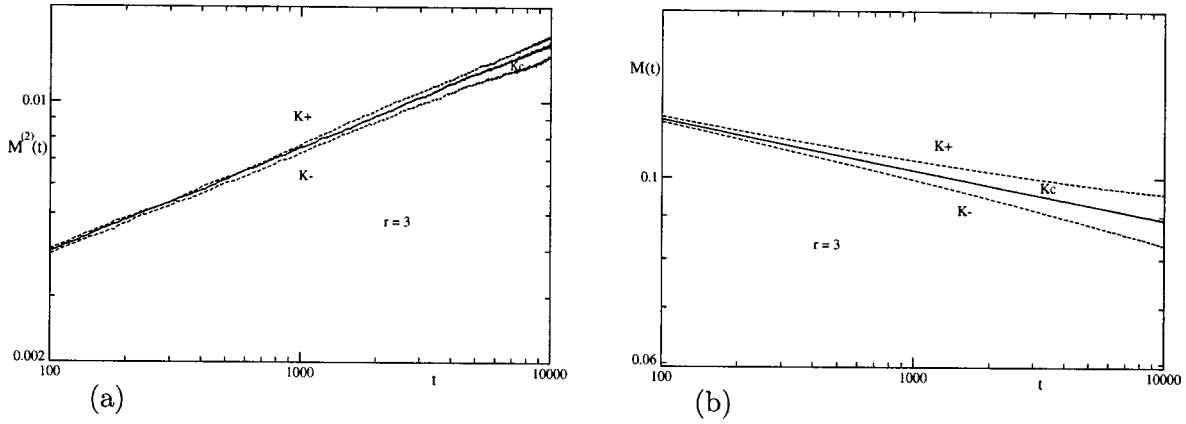


FIG. 1. The second-order phase transition induced by disorder at the disorder amplitude $r=3$. (a) The initial condition is completely disordered. The second moment $M^{(2)}(t)$ is plotted vs t on a log-log scale for $K_+=0.721\,525$, $K_c=0.717\,936$, and $K_-=0.714\,346$ with $L=280$. (b) The initial condition is completely ordered. The magnetization $M(t)$ is plotted vs t on a log-log scale for $K_+=0.721\,525$, $K_c=0.717\,936$, and $K_-=0.715\,064$ with $L=280$. Obviously, in both cases the observables reach a power-law behavior at the transition point K_c .

B. Quench with disorder start

Now let us concentrate our attention on the dynamic process with a completely disordered initial state. In Fig. 2, the second moment and autocorrelation with a disordered start are displayed for $r=3, 4$ and 10 with solid lines on a log-log scale. For the second moment, a power-law behavior is observed after a microscopic time scale $t_{mic} \sim 100$ or 200 Monte Carlo time steps. Corrections to scaling and the crossover effects are negligibly small even for $r=3$.

For the autocorrelation, there are some corrections to scaling or crossover effects for $r=3, 4$ up to a time around $t_{mic} \sim 800$. For $r=10$, however, a nearly perfect power-law behavior is seen starting from $t_{mic} \sim 200$.

In order to further confirm our results, some simulations up to a maximum time $150\,000$ have been performed and the samples for an average are 3000 . In Fig. 3(a), the autocorrelation is displayed. The power-law behavior is convincingly extended.

In Table I, the indices y and λ in Eqs. (14) and (15) measured from Fig. 2 are listed. If we may obtain the critical

exponent θ in some ways—e.g., from a dynamic evolution corresponding to Eq. (17)—we will be able to estimate both the dynamic exponent z and the static exponent β/ν from y and λ , respectively. In Ref. [18], an effort was made to measure the exponent θ . However, the obtained values are not compatible with our simulations. In other words, if we take the value of $\theta=0.203$ for $r=10$ from there, the resulting dynamic exponent z and static exponent β/ν are not consistent with other measurements in this paper and in simulations in equilibrium.

In Ref. [18], the magnetization (order parameter) is defined as the maximum value of the eight components of the Potts spin. This definition is good in simulations in equilibrium, since it help reduce the errors. However, it becomes problematic in a nonequilibrium state with a *specialized direction*—e.g., starting from an initial magnetization $m_0 = 1.0$ or a small but nonzero initial value in a certain component of the Potts spin. Actually, with this definition of the magnetization, its dynamic evolution does not depends on whether a small nonzero initial value at a certain direction of

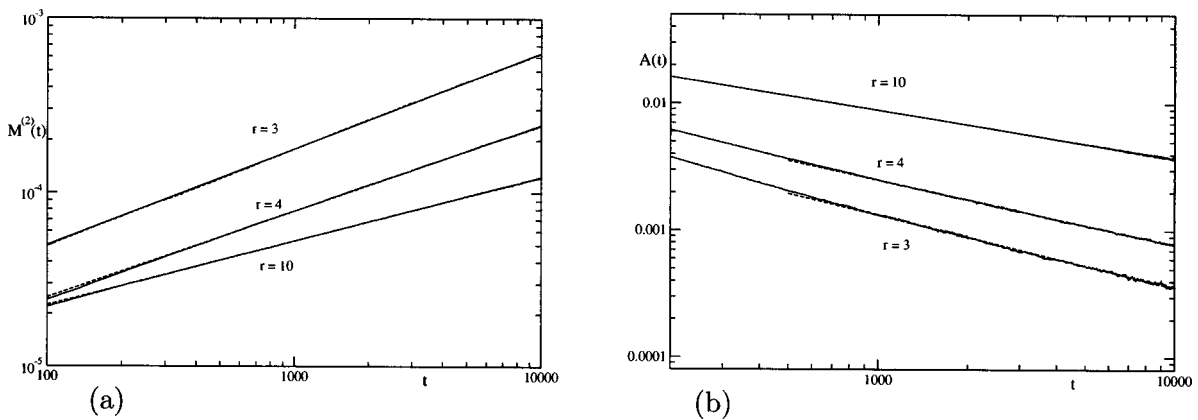


FIG. 2. The second moment and autocorrelation at the transition temperature with a disordered start. (a) $M^{(2)}(t)$ plotted vs t on a log-log scale. Solid lines are from numerical data with a lattice size $L=280$. Dashed lines show the power-law fits. For clarity, the data of $r=3$ have been shifted up by a factor of 2. (b) $A(t)$ plotted vs t on a log-log scale. Solid lines are from numerical data with a lattice size $L=280$. Dashed lines show the power-law fits.

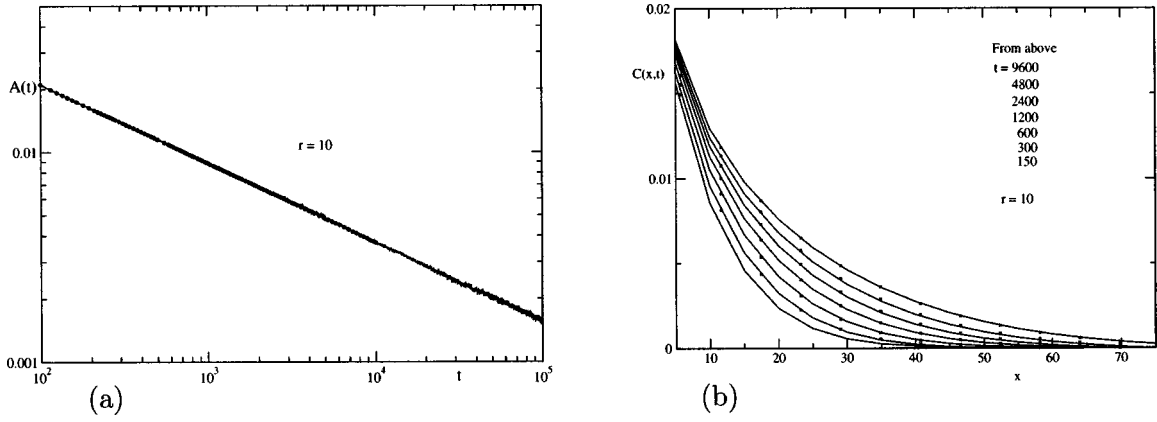


FIG. 3. (a) The autocorrelation with an disorder start for $r=10$ plotted vs t on a log-log scale. The lattice size is $L=280$. The solid line is with 3000 samples, and the circled line is the same as that in Fig. 2(b). (b) Data collapse of the correlation function $C(x,t)$ with a disordered start. Solid lines are for $t=150, 300, 600, 1200, 2400, 4800, 9600$ (from below). Crosses fitted to the curve at a time t are the data at $t/2$, but rescaled suitably according to Eq. (16) with $z=4.57$, $\beta/\nu=0.157$.

the Potts spin is given, and it *always* increases as time evolves.

With our definition of the magnetization, we have also tried to simulate the dynamic process starting from a disordered state but with a small nonzero initial magnetization. It turns out that the magnetization drops to zero already in an early time. This usually indicates that the exponent θ is very

TABLE I. The critical exponents of the 2D eight-state RBP model with different disorder amplitude r , measured from the scaling functions of $A(t)$, $M^{(2)}(t)$, $M(t)$, $\partial_\tau \ln M(t, \tau)$ and $U(t)$, respectively, starting from both the ordered and disordered initial states. Some results in the literature are also listed for comparison. The results of [17] are obtained with a self-dual continuous distribution of the couplings, which may be considered corresponding to a *big* r .

Exponent	m_0	$r=3$	$r=4$	$r=10$
$\lambda=d/z-\theta$	0.0	0.572(3)	0.508(5)	0.376(3)
$y=(d-2\beta/\nu)/z$		0.552(2)	0.496(2)	0.369(1)
$c_1=\beta/\nu z$	1.0	0.0560(4)	0.0485(5)	0.0343(2)
$c_1=1/\nu z$		0.438(9)	0.373(8)	0.226(5)
$c_2=d/z$		0.669(8)	0.593(4)	0.428(6)
$z=d/c_2$		2.99(4)	3.37(3)	4.67(7)
$\beta/\nu=(d-yz)/2$		0.169(9)	0.163(6)	0.156(11)
$z=d/(y+2c_1)$		3.01(2)	3.37(2)	4.57(2)
$\beta/\nu=c_1 z$		0.169(2)	0.164(2)	0.157(2)
$1/\nu=c_1 z$		1.32(3)	1.26(3)	1.03(3)
$\theta=d/z-\lambda$		0.092(5)	0.085(6)	0.061(4)
β/ν				0.160(4) [17]
$1/\nu$				1.01(2) [17]
y				0.438(6) [18]
c_1				0.0390(6) [18]
c_2				0.518(9) [18]
θ				0.203(3) [18]

close to zero or negative. Indeed, according to our estimation in the next subsection (see Table I), $\theta=0.092(5)$, $0.085(6)$, and $0.061(4)$ for $r=3, 4$, and 10 , respectively, apparently much smaller than $\theta=0.353(6)$, $0.262(4)$, and $0.203(3)$ for $r=2, 5$, and 10 estimated in Ref. [18]. However, from some other examples [31,32,45], $\theta=0.092$ seems not that small to be detected. This point remains a little puzzling. Probably, it might be related to the disorder or many components of the Potts spin.

To further clarify the the dynamic scaling behavior, we examine the spatial correlation function $C(x,t)$ and plot the data collapse for $r=10$ in Fig. 3(b). According to Eq. (16), the spatial correlation function at different times may collapse onto each other if x and $C(x,t)$ are rescaled suitably with the exponent z and $\beta/\nu z$. This is indeed the case as shown in Fig. 3(b). The values $z=4.57$ and $\beta/\nu=0.157$ used here will be confirmed in the next subsection.

C. Quench with ordered start

To complete our study and provide estimates of all the critical exponents, we now turn to a dynamic process starting from a completely ordered state—i.e., $m_0=1.0$. The fluctuation of the dynamic variables in this process is less than that with a disordered start. However, the dynamic evolution is somewhat slower and corrections to scaling are also relatively stronger.

In Fig. 4, the magnetization and Binder cumulant of $r=3, 4$ with an ordered start are displayed with solid lines on a log-log scale. The corrections to scaling or crossover effects are visible up to around $t_{mic} \sim 1000$. If one measures the exponents c_1 and c_2 , up to only a few hundred Monte Carlo time steps, there will be a discrepancy of about 20%.

For $r=10$, the corrections to scaling are somewhat less but still not negligible within some hundred time steps. In order to make our results more convincing, as an example, we have performed the simulations for $r=10$ up to a maximum time $t=150\,000$. This is shown in Fig. 5.

In Table I, the estimated values of c_1 and c_2 are given in comparison with those from Ref. [18]. The discrepancy be-

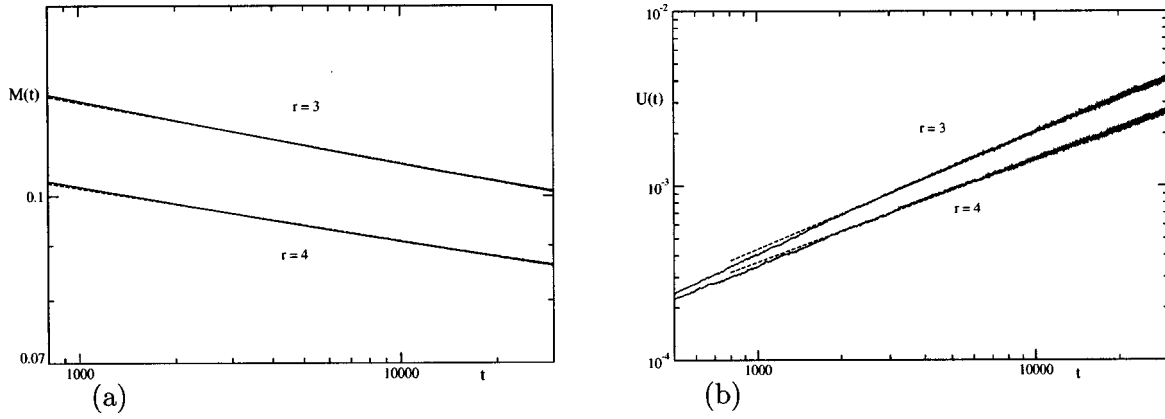


FIG. 4. The magnetization and Binder cumulant with an ordered start. (a) $M(t)$ plotted vs t on a log-log scale. Solid lines are for $r=3$ and 4 with a lattice size $L=280$. Dashed lines show the power-law fits. For clarity, the curve of $r=3$ has been shifted up by a factor of 1.2. (b) $U(t)$ plotted vs t on a log-log scale. Solid lines are for $r=3$ and 4 with a lattice size $L=280$. Dashed lines show the power-law fits.

tween our results and those of Ref. [18] is about 15%–20%. The errors in Table I are not only statistical errors. In some cases, errors induced by corrections to scaling have been taken into account when they are comparable or bigger than statistical errors. To achieve even more accurate results, in principle, we may think about to introduce some ansatz to describe the corrections to scaling—e.g., as done in Ref. [46]. However, we could not succeed, probably because the corrections to scaling are somewhat strong and the four- (or more-) parameter fit is not stable or we have not found a correct ansatz.

Finally, we perform simulations at temperatures around the transition point to approximate the differentiation of $\ln M(t, \tau)$. Then we may estimate the index $c_1 = 1/\nu z$ from Eq. (10). The curves are plotted in Fig. 6. As usual, some extra corrections may arise from the approximation of a differentiation with a difference, and the errors are also a little bigger than those of other observables. Taking into account that it is not so easy to estimate the exponent ν , we are satisfied at moment with our results.

In the first sector of Table I, we summarize all our measurements of the indices λ , y , c_1 , c_l and c_2 . Since we are about to determine four critical exponents z , β/ν , $1/\nu$ and θ

from these five independent measurements of the indices, we may have different ways to do it.

(1) From c_2 , we may independently estimate the dynamic exponent z . With z as an input, we obtain the static exponents β/ν and $1/\nu$ and the dynamic exponent θ from c_1 , c_l and λ respectively. The measurement of y provides an independent check of the exponent β/ν .

(2) We forget about c_2 , and determine z from y and c_1 , and then proceed to estimate other exponents β/ν , $1/\nu$ and θ from c_1 , c_l , and λ , respectively.

The results of the second approach and a part of the results of the first approach are given in the second sector of Table I. The third sector includes some measurements in Refs. [17,18] for comparison. In Ref. [17], simulations are performed for a self-dual continuous distribution of the couplings, and it may be considered corresponding to a *big* r .

In Table I, we may first observe that different methods for estimating z and β/ν yield consistent results within the errors. This provides us confidence that our results are reliable. However, the determination of z from y and c_1 is more accurate. Therefore, it is used for calculating β/ν , $1/\nu$, and θ —i.e., following the second approach above. In addition, we should mention that the error of β/ν estimated from c_1 is

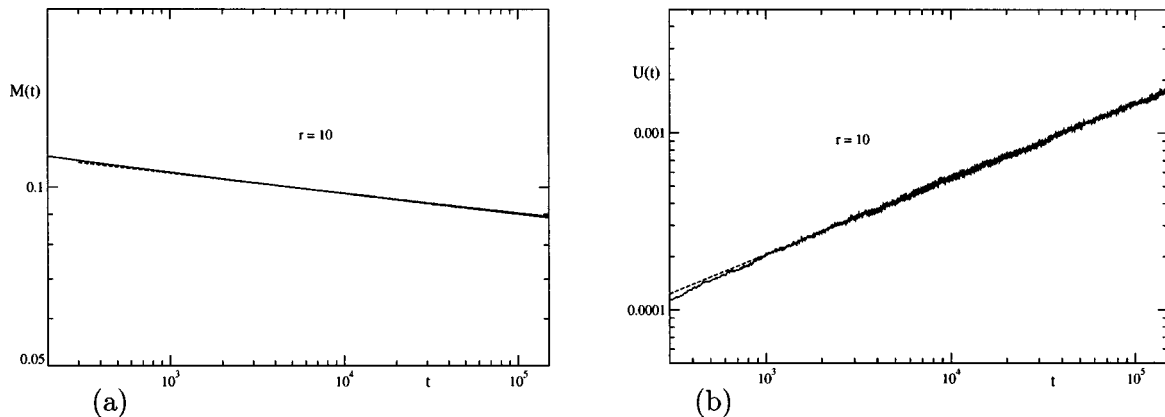


FIG. 5. The magnetization and Binder cumulant with an ordered start for $r=10$. (a) $M(t)$ plotted vs t on a log-log scale. The solid line is obtained with a lattice size $L=280$, and the dashed line shows the power-law fit. (b) $U(t)$ plotted vs t on a log-log scale. The solid line is obtained with a lattice size $L=280$ and the dashed line shows the power-law fit.

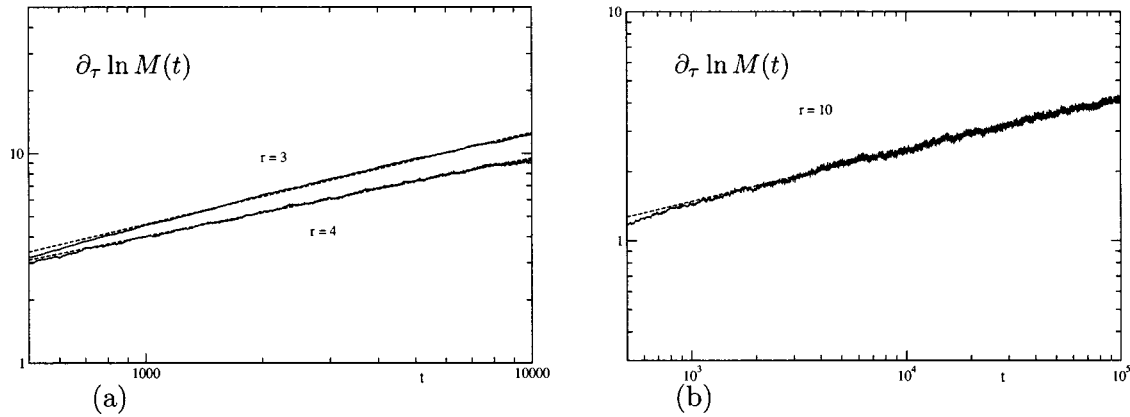


FIG. 6. $\partial_\tau \ln M(t)$ plotted vs t on a log-log scale with an ordered start. (a) Solid lines are for $r=3$ and 4 with a lattice size $L=280$. Dashed lines show the power-law fits. (b) The solid line is for $r=10$ with a lattice size $L=280$ and the dashed line shows the power-law fit.

smaller than that from y . This is because in the latter case β/ν is expressed as a difference of d and yz , and both d and yz are much bigger than β/ν .

On the other hand, β/ν shows little dependence on the disorder amplitude r . This is consistent with the results in Refs. [15,16]. The value $\beta/\nu=0.157(2)$ for $r=10$ is in good agreement with $\beta/\nu=0.153(3)$ for $r=10$ in Ref. [27] and $\beta/\nu=0.160(4)$ for a *big* r in Ref. [17], and clearly different from $\beta/\nu=0.125$ of the 2D Ising model.

Our values of $1/\nu$ show a visible dependence on r . It is qualitatively similar to the numerical results for the three-state RBP model [15]. This kind of phenomenon seems to be typical for physical systems with disorder. As r increases, $1/\nu$ tends to 1.0, the Ising value in two dimensions. Such trend is also reported for a *big* r in Ref. [17].

Another new result in our simulations is the estimate of the dynamic exponent z . With disorder, the dynamic exponent z depends on the disorder amplitude r and is significantly bigger than $z=2.165$ of the 2D dynamic Ising model [32,38]. For $r=10$, the value $z=4.57$ indicates that the dynamics is rather slow. It is clear that the 2D dynamic RBP model is not in the same dynamic universality class as the 2D dynamic Ising model. Further evidence is the small values of θ from 0.061 to 0.092, compared with $\theta=0.191$ of the 2D Ising model [32,47].

Comparing our results for $r=10$ with those in Ref. [18], one finds a discrepancy of 15%–20% for the indices y , c_1 , and c_2 , while the measurement of θ in Ref. [18] seems problematic. Theoretically, the exponent θ governs the initial increase of the magnetization in Eq. (17). In Ref. [18], the magnetization is defined as the maximum value of the eight components of the Potts spin. Even if the initial magnetization is set to $m_0=0$, the magnetization with that definition will increase. Therefore, the resulting exponent does not correspond to θ , and it is rather close to $(d-2\beta/\nu)/2z$. For the case of $m_0=0$, the definitions of the magnetization in Ref.

[18] and in the present paper yield almost the same results, since there are no specialized directions of the Potts spins in the dynamic process. For the case of $m_0=1$, there is some difference between two definitions of the magnetization, but it is not significant (about 2%–3% within our simulations), since the component of the Potts spin with $m_0=1$ dominates the dynamic process. Therefore, the discrepancy of 15%–20% for the indices y , c_1 , and c_2 in Ref. [18] is mainly from corrections to scaling induced by disorder.

IV. CONCLUSION

In conclusion, with large-scale Monte Carlo simulations we have investigated the critical dynamic behavior in non-equilibrium dynamic processes starting from both ordered and disordered states for the two-dimensional eight-state random-bond Potts model. With the dynamic approach, a second-order phase transition is confirmed and the dynamic scaling behavior far from equilibrium is systematically verified. Both the dynamic and static critical exponents are estimated with relatively good accuracy.

The static exponent β/ν shows little dependence on the disorder amplitude r , and its value $\beta/\nu=0.157(2)$ for $r=10$ is in agreement with that in Refs. [17,27]. The dynamic exponent z and static exponent $1/\nu$ vary with the strength of disorder. This scenario is similar to that of $1/\nu$ in the three-state RBP model [15]. The dynamic exponent z is much bigger than that of the 2D Ising model. The exponent θ estimated indirectly in this paper is much smaller than that in Ref. [18].

ACKNOWLEDGMENTS

This work was supported in part by NNSF (China) under Grant Nos. 10325520 and 10275054 and by SRFDP (China) and DFG (Germany) under Grant No. TR 300/3-3.

- [1] A. B. Harris, *J. Phys. C* **7**, 1671 (1974).
- [2] Y. Imry and M. Wortis, *Phys. Rev. B* **19**, 3580 (1979).
- [3] K. Hui and A. N. Berker, *Phys. Rev. Lett.* **62**, 2507 (1989).
- [4] M. Aizenman and J. Wehr, *Phys. Rev. Lett.* **62**, 2503 (1989).
- [5] S. Chen, A. M. Ferrenberg, and D. P. Landau, *Phys. Rev. Lett.* **69**, 1213 (1992).
- [6] S. Chen, A. M. Ferrenberg, and D. P. Landau, *Phys. Rev. E* **52**, 1377 (1995).
- [7] S. Wiseman and E. Domany, *Phys. Rev. E* **51**, 3074 (1995).
- [8] L. Schwenger, K. Budde, C. Voges, and H. Pfñür, *Phys. Rev. Lett.* **73**, 296 (1994).
- [9] A. W. W. Ludwig, *Nucl. Phys. B* **330**, 639 (1990).
- [10] V. Dotsenko, M. Picco, and P. Pujol, *Nucl. Phys. B* **455**, 701 (1995).
- [11] H. Chate, Q. H. Chen, and L. H. Tang, *Phys. Rev. Lett.* **81**, 5471 (1998).
- [12] J. Cardy, *J. Phys. A* **29**, 1897 (1996).
- [13] J. Cardy and J. L. Jacobsen, *Phys. Rev. Lett.* **79**, 4063 (1997).
- [14] Ricardo Paredes V. and J. Valbuena, *Phys. Rev. E* **59**, 6275 (1999).
- [15] J. K. Kim, *Phys. Rev. B* **53**, 3388 (1996).
- [16] M. Picco, *Phys. Rev. B* **54**, 14930 (1996).
- [17] T. Olson and A. P. Young, *Phys. Rev. B* **60**, 3428 (1999).
- [18] H. P. Ying and K. Harada, *Phys. Rev. E* **62**, 174 (2000).
- [19] F. Yasar, Y. Gündüç, and T. Celik, *Phys. Rev. E* **58**, 4210 (1998).
- [20] C. Chatelain and B. Berche, *Nucl. Phys. B* **572[FS]**, 626 (2000).
- [21] J-Ch. Anglés d'Auriac and F. Iglói, *Phys. Rev. Lett.* **90**, 190601 (2003).
- [22] J. L. Jacobsen and J. Cardy, *Nucl. Phys. B* **515**, 701 (1998).
- [23] C. Chatelain, B. Berche, W. Janke, and P. E. Berche, *Phys. Rev. E* **64**, 036120 (2001).
- [24] A. Oosawa and H. Tanaka, *Phys. Rev. B* **65**, 184437 (2002).
- [25] C. Deroulers and A. P. Young, *Phys. Rev. B* **66**, 014438 (2002).
- [26] W. Janke and M. Weigel, *Phys. Rev. B* **69**, 144208 (2004).
- [27] C. Chatelain and B. Berche, *Phys. Rev. Lett.* **80**, 1670 (1998).
- [28] F. Y. Wu, *Rev. Mod. Phys.* **54**, 235 (1982).
- [29] H. K. Janssen, B. Schaub, and B. Schmittmann, *Z. Phys. B: Condens. Matter* **73**, 539 (1989).
- [30] D. A. Huse, *Phys. Rev. B* **40**, 304 (1989).
- [31] Z. B. Li, U. Ritschel, and B. Zheng, *J. Phys. A* **27**, L837 (1994).
- [32] B. Zheng, *Int. J. Mod. Phys. B* **12**, 1419 (1998), review article.
- [33] K. Humayun and A. J. Bray, *J. Phys. A* **24**, 1915 (1991).
- [34] B. Zheng, M. Schulz, and S. Trimper, *Phys. Rev. Lett.* **82**, 1891 (1999).
- [35] H. K. Janssen, in *From Phase Transition to Chaos*, edited by G. Györgyi, I. Kondor, L. Sasvári, and T. Tél, Topics in Modern Statistical Physics (World Scientific, Singapore, 1992).
- [36] H. J. Luo, L. Schülke, and B. Zheng, *Mod. Phys. Lett. B* **13**, 417 (1999).
- [37] D. Stauffer, *Physica A* **186**, 197 (1992).
- [38] N. Ito, *Physica A* **196**, 591 (1993).
- [39] B. Zheng, in *Computer Simulation Studies in Condensed-Matter Physics XVII*, edited by D. P. Landau (Springer, Heidelberg, 2004).
- [40] H. J. Luo, L. Schülke, and B. Zheng, *Phys. Rev. Lett.* **81**, 180 (1998).
- [41] N. Ito and Y. Ozeki, *Physica A* **321**, 262 (2003).
- [42] W. Kinzel and E. Domany, *Phys. Rev. B* **23**, 3421 (1981).
- [43] T. Celik, F. Yasar, and Y. Gündüç, *Comput. Phys. Commun.* **121-122**, 194 (1999).
- [44] L. Schülke and B. Zheng, *Phys. Rev. E* **62**, 7482 (2000).
- [45] L. Schülke and B. Zheng, *Phys. Lett. A* **204**, 295 (1995).
- [46] A. Jaster, J. Mainville, L. Schülke, and B. Zheng, *J. Appl. Phys.* **32**, 1395 (1999).
- [47] P. Grassberger, *Physica A* **214**, 547 (1995).